Journal of Statistical Physics, Vol. 88, Nos. 3/4, 1997

Kolmogorov–Sinai Entropy, Lyapunov Exponents, and Mean Free Time in Billiard Systems

P. L. Garrido[1]

Received April 3, 1995; final February 19, 1997

We perform new experiments on the Kolmogorov–Sinai entropy, Lyapunov exponents, and the mean free time in billiards. We study their dependence on the geometry of the scatterers made up of two interpenetrating square lattices, each one with circular scatterers with different radius. We find, in particular, that the above quantities are continuous functions of the ratio of the scatterer radius. However, it seems that their derivative is discontinuous around the radius ratio which separates the diffusive and nondiffusive types of geometries.

KEY WORDS: Billiards; Kolmogorov–Sinai entropy; Lyapunov exponents; ergodic theory; chaos; numerical experiments.

1. INTRODUCTION, SOME DEFINITIONS AND PREVIOUS RESULTS

Dispersing billiards are extremely useful models to study dynamical properties which are present in many other non-dissipative systems. Beyond their physical relevance, their simple definition make them natural candidates to develop and/or to apply rigorous mathematical tools. On the other hand, their simplicity make it also possible to study their behavior by careful computer experiments whose results may shed new light on some unsolved conjectures and/or proofs. The interaction between mathematical physics and computer experiments has been extremely fruitful in this particular case.

In this paper we extend and complete a previous computer experiment about billiards.[1] Our goal is to study the influence of the *geometry*

[1] Instituto Carlos I de Física Teórica y Computacional, Facultad de Ciencias, Universidad de Granada, 18071-Granada, Spain.

0022-4715/97/0800-0807$12.50/0

822/88/3-4-18

of scatterers on the billiard behavior. We mean here by *geometry* of the scatterers whether there are collisionless trajectories (billiards *with horizon* denoted by ∞H), or not (billiards *without horizon*, denoted 0H), when the periodicity of the obstacles does not allow one to draw a path to infinity avoiding the obstacles, or *diamond* billiards, denoted D, in the other case where the obstacles keep the particle inside a bounded region. In particular we study the Kolmogorov–Sinai entropy which is related to the number of symbols necessary for an optimal coding of the particle trajectory, the Lyapunov exponents which define the time-scale of the systems chaoticity and the mean free time between collisions. The latter is used to check the goodness of the computer simulation by comparing the mean free time numerical results with its well known analytic formula.

In order to get an analytic expression for the KS entropy of the Sinai billiard, we need more detailed information about the dynamics (see basic definitions in ref. 2). The two dimensional phase space consists of points $x=(r, \Phi)$ where r represents the position of the particle when it hits an obstacle and $\Phi \in (\pi/2, 3\pi/2)$ is the incident angle formed by the velocity at collision and the outer normal to the obstacle, measured counterclockwise. The dynamics is the map T mapping one collision $x=(r, \Phi)$ to the previous one $x'=(r', \Phi')$. In fact, it is simple to show that an initial curve in the phase space, $(r', \Phi'(r'))$, after one collision it becomes $(r, \Phi(r))$ where both curves are related by the differential equation:

$$\frac{1}{-\cos\Phi}\frac{d\Phi}{dr}=\frac{\kappa(r)}{-\cos\Phi}+\cfrac{1}{\tau+\cfrac{1}{\cfrac{1}{-\cos\Phi'}\cfrac{d\Phi'}{dr'}+\cfrac{\kappa(r')}{-\cos\Phi'}}} \tag{1.1}$$

valid at every point of the curve where the map T has no singularity, here $\kappa(r)$ is the obstacle curvature at point r and τ is the distance between the collision points x and x'. By iterating the equation (1.1) an initial segment

$$\Phi^{(0)}(r_0)=\int_{r_0}^{r_0+\delta}\kappa(r)\,dr \tag{1.2}$$

where δ is assumed to be suitable small, becomes the solution of the differential equation:

$$\frac{1}{-\cos\Phi^{(n)}}\frac{d\Phi^{(n)}}{dr^{(n)}}=\frac{\kappa(r^{(n)})}{-\cos\Phi^{(n)}}+B(n) \tag{1.3}$$

where we set $x \equiv x^{(n)} = (r^{(n)}, \Phi^{(n)}) \equiv T^{-n}(T^n x)$ and $x^{(j)} = T^{-j}(T^n x)$ and where $r^{(j)}$ and $\Phi^{(j)}$ are the phase space coordinates after then jth collision trajectory $x^{(n)}, \ldots, x^{(0)}$, and:

$$B(n) = \cfrac{1}{\tau(n-1,n) + \cfrac{1}{\cfrac{-2\kappa(r^{(n-1)})}{\cos \Phi^{(n-1)}} + B(n-1)}} \tag{1.4}$$

with $B(0) = 1$ and $\tau(n-1, n)$ is the distance between collisions $n-1$ and n, and $B(n)$ depends on x see ref. 2, p. 244. We have also assumed that the map T is not singular along the trajectory $x^{(0)}, \ldots, x^{(n)}$.

The Kolmogorov–Sinai Entropy is then proved in ref. 3 to be given by the integral over phase space:

$$h(T) = \int \nu(dx) \log \det \partial T_e(x) \tag{1.5}$$

where T_e is the restriction of the map T to the unstable manifold in x and ν is the invariant measure under T given by: $d\nu(x) = -(2P)^{-1} \cos(\Phi)\, dr\, d\Phi$ where P is the total perimeter of the obstacles.

In fact suppose that $\gamma'(x') = T\gamma(x)$, $\gamma \equiv T^{-1}\gamma'$, if γ', γ are two increasing curves around $x' = Tx$ and x, i.e., $d\Phi/dr > 0$ and $d\Phi'/dr' > 0$. Then the expansion rate at x' (using as metric $dr^2 + \kappa^{-2} d\Phi^2$ and setting $c \equiv \cos \Phi$, $c' = \cos \Phi'$, $\kappa = \kappa(r)$, $\kappa' = \kappa(r')$) is:

$$\frac{d\,|T^{-1}\gamma'|}{d\gamma'} = \frac{-c'}{-c} \frac{(\kappa^{-2}(d\Phi/dr)^2 + 1)^{1/2}}{(\kappa'^{-2}(d\Phi'/dr')^2 + 1)^{1/2}} \left(1 + \tau(T^{-1}x') \frac{1}{-c'} \left(\kappa' + \frac{d\Phi'}{dr'}\right)\right) \tag{1.6}$$

having used the elementary trigonometrical relations in ref. 2, p. 244; so that using that $\int \nu(dx)(F(x) - F(Tx)) \equiv 0$ by the invariance of $\nu(dx)$ we get:

$$\begin{aligned} h(T^{-1}) &= \int \nu(dx') \log \left(1 + \frac{\tau(T^{-1}x')}{-c} \left(\kappa' + \frac{d\varphi'}{dr'}\right)\right) \\ &= \int \nu(dx) \log(1 + \tau(T^{-1}x)\, \tilde{B}_e(x)) \end{aligned} \tag{1.7}$$

having renamed x' with x in the second step, which also defines $\tilde{B}_e(x)$. A rigorous proof of the above derivation of $h(T)$ can be found in ref. 4.

On the other hand the equation $\varphi = \varphi(r)$ of the expanding manifold $\gamma_e(x)$, which is easily seen to be a monotonically increasing function of r (see ref. 2), can be obtained from the relation:

$$\gamma_e(x) = \lim_{n \to \infty} T^{-n} \gamma_e^0(T^n x) \tag{1.8}$$

if γ_e^0 is the curve with equation $d\varphi/dr = 0$ (or equal to any monotonically increasing function, arbitrarily prefixed), see ref. 2.

It is convenient to define, setting $c_n \equiv \cos \Phi^{(n)}$, $\kappa_n = \kappa(r^{(n)})$:

$$B(j) = \tilde{B}(j) - \frac{2\kappa_n}{-c_n} \tag{1.9}$$

and it is easily checked, ref. 2, p. 744, that $B(n)$ coincides with (1.4).

Hence:

$$h(T^{-1}) = \lim_{n \to \infty} \int d\nu(x^{(n)}) \ln \left(1 + \tau(n, n+1) \left(B(n) + \frac{2\kappa_n}{-c_n} \right) \right) \tag{1.10}$$

A different way to compute the KS entropy is to use the *Pesin identity*:

$$h(S^{-1}) = \sum_{\lambda_i > 0} \lambda_i \tag{1.11}$$

with the *Abramov formula*:

$$h(S^{-1}) = \frac{h(T^{-1})}{\tau} \tag{1.12}$$

where S is the billiard flow, τ is the mean free time between collisions and λ_i are the system Lyapunov exponents. In the Sinai Billiard case, there is only one positive Lyapunov exponent λ and then it is proportional to the KS entropy. The Lyapunov exponent λ can be computed directly by using its definition (see ref. 5 for more details):

$$\lambda = \lim_{n \to \infty} \frac{1}{n} \ln |C(n)\, \psi| \tag{1.13}$$

where $C(n) = A(n, n-1)\, A(n-1, n-2) \cdots A(1, 0)$,

$$A(m+1, m) = \begin{pmatrix} \dfrac{R(m+1)[rcs(m) + \tau(m, m+1)]}{R(m)\, rcs(m+1)} & \dfrac{R(m)\, R(m+1)\, \tau(m, m+1)}{rcs(m)\, rcs(m+1)} \\ \dfrac{\tau(m, m+1) + rcs(m) + rcs(m+1)}{R(m)\, R(m+1)} & \dfrac{R(m)[rcs(m+1) + \tau(m, m+1)]}{R(m+1)\, rcs(m)} \end{pmatrix} \tag{1.14}$$

$rcs(m) = -R(m) \cos \Phi(m)$, $R(m)$ is the radius of the obstacle at the mth hit and ψ is any initial vector $\psi = (r, \sin \Phi)$.

Some numerical results about the KS entropy, the Lyapunov exponents and the mean free time is available in the literature. Let us make a brief report.

Benettin and Strelcyn[6] found in 1978 numerical evidence that the KS entropy of a generalized stadium billiard is not a monotone decreasing function of a topological parameter δ which controls the stadium curvature.

In 1984 Benettin[5] studied numerically the Lyapunov exponent for the Diamond billiard as a function of the sides curvature, ε. He found that the behavior $h \simeq \varepsilon^{1/2}$ fitted his results very well for all data between $0 < \varepsilon < 1$.

Also, in 1984, Friedman, Oono add Kubo,[7] studied numerically and analytically the KS entropy for a two dimensional square and triangular lattice billiards when the radius, R, tend to zero. Thet found that $h \simeq -2 \ln R$ when $R \to 0$. They also studied the triangular billiard around the critical radius which Separates the finite horizon behavior from the infinite horizon one. They claimed, without showing it, that the KS entropy is continuous and they suggested that it is even continuously differentiable..

In 1985 Bouchaud and Le Doussal[8] studied numerically the KS entropy for a two dimensional square lattice billiard. They confirmed the small R behavior found by Friedman *et al.*,[7] in particular they got $h \simeq \alpha \log \beta/R$ with $\alpha \simeq \beta = 2 \pm 0.2$. They also found that h grows regularly for $R = 0$ until $R \simeq 1$, which is the critical value which separates the infinite horizon behavior from the diamond one. They argue that $h \simeq (1-R)^{1/2}$ when $R \to 1^-$ but they do not confirm this point with their numerical experiment. In fact, they observe a quasiconstant value of $h(S)$ between $R = 0.99$ and $R = 0.999$, before the steep decrease when R is very close to 1.

Finally let us mention the works of P. R. Baldwin in 1988 and 1991.[9, 10] In the first one he studied numerically an infinite horizon soft billiard system (i.e., the scatterers are regions with a constant potential, U).

In particular, he argued that $h \simeq \ln U/R^2$ when $R^2 \ll U \ll 1$. More interesting is his 1991 work where he manage to give an explicit encoding for the trajectories of a particle in the ∞H billiard which is near the optimal one. He computes and confirms the KS entropy results of Friedman *et al.* [7] when $R \to 0$ by studying smaller radius than them.

2. THE COMPUTER EXPERIMENT

Our system is a square with periodic boundary conditions with sides of unit length, $a = 1$. We take the center of the torus as the origin of coordinates: (0, 0). There are a circle of radius R and center at (0, 0) and four more circles with radius R' and centers at (1/2, 1/2), (1/2, −1/2), (−1/2, −1/2), (−1/2, 1/2). Obviously only the part of the circles inside the torus is relevant (see Fig. 1).

A point particle is moving freely with unit velocity, $|v| = 1$, in the space external to the circles and hitting them elastically (conserving the modulus of the total momentum and the energy).

For any fixed $R' < 1/\sqrt{2}$ there are four different regions in the R parameter space (see Fig. 2):

- (T) Triangle: $1/2 \leqslant R \leqslant \sqrt{1/2 - R' + R'^2}$.
- (D) Diamond: $1/\sqrt{2} - R' \leqslant R \leqslant 1/2$.
- $(0H)$ Billiards without horizon: $1/2 - R' \leqslant R \leqslant 1/\sqrt{2} - R'$.
- (∞H) Billiards with infinite horizon: $0 \leqslant R \leqslant 1/2 - R'$.

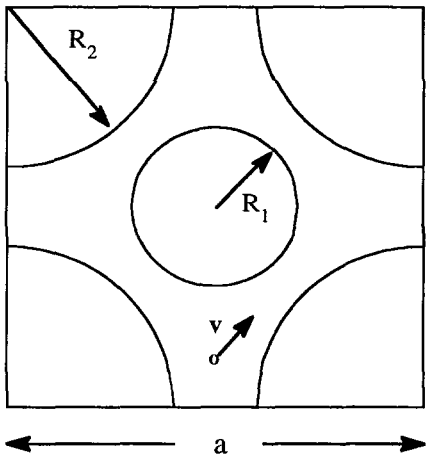

Fig. 1. General billiard structure with scatterers of radius R and R' in a box with side length a.

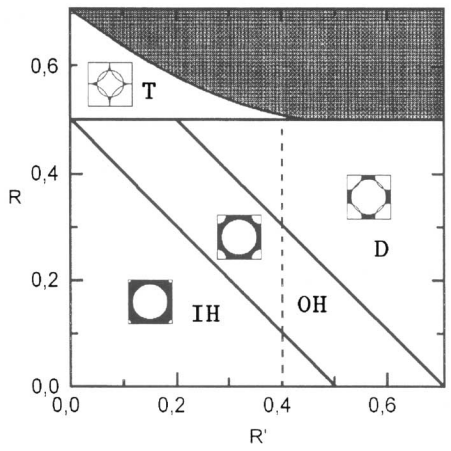

Fig. 2. Four possible billiard configurations for different R and R' values. Scatterers cover the full space in the gray zone. All the (R, R') values studied in this paper are located along the dashed line.

In this paper we fix $R' = 0.4$. Therefore the regions become: T: $0.5 \leqslant R \leqslant 0.509901...$; D: $0.307107... \leqslant R \leqslant 0.5$; $0H$: $0.1 \leqslant R \leqslant 0.307107...$; ∞H: $0 \leqslant R \leqslant 0.1$. We compute the different observables we explain below on the regions D, $0H$ and ∞H as a function of R. Region T is so small, in this case, that our algorithm becomes very unefficient in CPU computer time, so we do not study it. The algorithm we use is explained with detail in Ref. 1.

For each radius R, we have computed the evolution of the following observables:

(a) *The curvature operator* (*Eq.* 1.4)):

$$B(n) = \frac{1}{N} \sum_{i=1}^{N} B_i(n) \tag{2.1}$$

(b) *The KS entropy* (*Eq.* (1.10)):

$$h(n) = \frac{1}{N} \sum_{i=1}^{N} \ln \left[1 + \tau_i(n, n+1) \left(B_i(n) + \frac{2\kappa_n^{(i)}}{-c_n^{(i)}} \right) \right] \tag{2.2}$$

(c) *The Lyapunov exponent*:

$$\lambda(n) = \frac{1}{Nn} \sum_{i=1}^{N} \ln |C_i(n)\, \psi| \tag{2.3}$$

Table I. Number of points $N(f)$ and final collision $n_{max}(f)$ that we have used to fit the evolution of the observables: $f=h$, B and L to be the function $f(n)=a_1+a_2n^{-a_3}$, where $n\in[n_{max}(f)-N(f), n_{max}(f)]$ is the collision number and R is the radius studied.

R	$N(h)$	$n_{max}(h)$	$N(B)$	$n_{max}(B)$	$N(L)$	$n_{max}(L)$
0.0000	10	17	7	17	9	17
0.0200	8	16	9	16	9	16
0.0400	9	16	8	16	9	16
0.0600	8	16	9	16	9	16
0.0800	9	16	9	17	9	16
0.1000	10	17	10	17	9	17
0.1200	10	17	10	17	9	17
0.1400	10	18	10	18	10	18
0.1600	10	18	11	19	10	18
0.1800	10	19	11	20	10	19
0.2000	11	20	12	21	11	20
0.2200	12	21	11	22	11	21
0.2400	13	23	13	23	12	23
0.2600	13	24	14	25	13	24
0.2800	14	25	14	25	13	25
0.3000	16	30	17	33	16	30
0.3010	16	31	17	33	16	31
0.3020	16	31	18	34	16	31
0.3030	16	31	18	34	16	31
0.3040	17	32	18	35	17	32
0.3050	17	32	18	35	17	32
0.3055	17	32	18	35	17	33
0.3060	17	32	19	36	17	33
0.3062	17	32	19	36	18	34
0.3065	18	34	18	34	18	34
0.3070	17	32	19	36	18	35
0.3072	17	32	19	36	19	37
0.3075	17	32	19	36	17	32
0.3080	7	31	18	35	10	40
0.3090	4	31	18	34	10	40
0.3100	6	30	18	34	10	40
0.3110	9	30	3	33	16	30
0.3120	7	30	7	33	16	30
0.3130	7	30	18	33	15	29
0.3140	12	30	18	33	15	29
0.3200	14	25	14	25	13	25
0.3400	8	25	9	25	13	25
0.3600	14	25	10	25	13	25
0.3800	16	30	14	30	15	29
0.4000	17	31	18	33	16	30
0.4200	16	30	13	30	16	30
0.4400	18	35	12	35	18	35
0.4600	6	39	21	40	21	40
0.4800	25	48	26	50	26	50

(d) *The mean free time*:

$$\tau = \frac{1}{N n_{col}} \sum_{i=1}^{N} \sum_{n=1}^{n_{col}} \tau_i(n-1, n) \tag{2.4}$$

Where N is the number trajectories with different random initial conditions and n_{col} is the number of collisions corresponding one trajectory. In our computer simulation $N = 10^7$ for all R and, in most of the cases $n_{col} = 50$. The different radius that we have studied in this paper appear on Table I. Let us remark that the error bars are included in all the figures showed below. Sometimes they do not appear explicitly because the symbol size is much bigger that the error bar size.

3. THE RESULTS

I. The Curvature Operator

Some typical averaged evolutions for the curvature operator $B(n)$ are presented in Fig. 3. We see that, depending on the radius, the convergence to an asymptotic value is reached after 5 to 15 collisions. In fact, we see that there is a kind of critical slowing down as we approach the critical radius $R_c = 0.307107...$ which separates the diamond topology and the $0H$

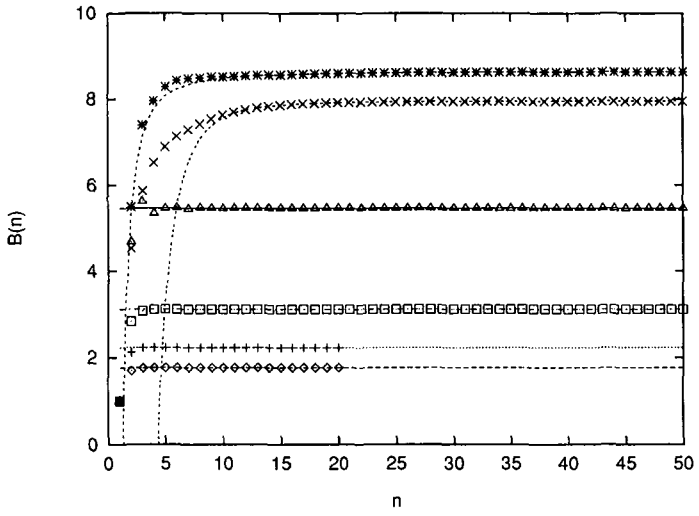

Fig. 3. $B(n)$ given by Eq. (1.4) as a function of n for different radius (from top to bottom): $R = 0.48, 0.30, 0.40, 0.20, 0.10$ and 0. The lines are the corresponding fits (see text).

one. This is so because for the critical radius case, R_c, the vertex of the diamond are tangent and then they are trajectories which may become trapped infinite time in their neighborhood. We are interested in the asymptotic value of $B(n)$ when $n \to \infty$. Because the system chaoticity and the initial rounding error propagation through the simulation, we should discard the data after some collisions.

In particular, we can estimate the maximum number of collisions that we may keep safely. We equate the data statistical error: $\sigma(B)/\sqrt{N}$, with the expected rounding error propagation after $n_{max}(R, B)$ collisions: $10^{-16} \exp[\lambda'(R)\, n_{max}(R, B)]$, where $\sigma(B)$ is the standard deviation for the B data, $\lambda(R)$ is a rough estimate of the Liapunov exponent and we have assumed that the initial error is 10^{-16} because we are working in double precision. This implies that $n_{max}(R, B) = \min\{[16 \ln(10) - \ln(N)/2 + \ln(\sigma(B))]/\lambda'(R), n_{col}(R)\}$. As we see in Fig. 3, for some values of R,. we observe a kind of slow decay and therefore, it is risky to identify $B(n_{max}(R, B))$ with the wanted asymptotic value $B = \lim_{n \to \infty} B(n)$. It is more convenient to study the data asymptotic behaviour. In order to do this, we have fitted $B(n)$ to the function

$$B(n) = a_1 + \frac{a_2}{n^{a_3}},\ n \in [n_0(B, R), n_{max}(R, B)] \tag{3.1}$$

where $n_0(B, R) = n_{max}(R, B)/2$.

Then the asymptotic value B is identified with the coefficient a_1. When the error bar for the coefficient a_1, σ_{a_1}, is such that $a_2/n_{max}(R, B)^{a_3} \leqslant \sigma_{a_1} \leqslant a_2/n_0(R, B)^{a_3}$, that is, when the fitted function variation over the interval is smaller than the typical error, we change the strategy. In this case, we define $n_0(R, B) = (|a_2|/\sigma_{a_1})^{1/a_3}$ and we take as asymptotic value the average of $B(n)$ over the interval $n \in [n_0(B, R), n_{max}(R, B)]$.

The asymptotic value $B = \lim_{n \to \infty} B(n)$, is plotted in Fig. 4. We see how the curvature operator behaves in the three regions. In the ∞H and $0H$ regions, B is an increasing function on R. In the D region B is a decreasing function on R when $R \leqslant 0.4$ and increasing one when $R \geqslant 0.4$. We fitted Several functions to these data. The best ones are:

(a) ∞H *interval* (6 *points*): $B(R) = b_1 + b_2 R$ where $b_1 = 1.76 \pm 0.01$ and $b_2 = 4.5 \pm 0.2$.

(b) $0H$ *interval* (20 *points*): $B(R) = b_1 + b_2 R + b_3 (R_c - R)^{-b_4}$ where $b_1 = -2.9 \pm 0.7$, $b_2 = 3.1 \pm 1.4$, $b_3 = 3.4 \pm 0.7$ and $b_4 = 0.21 \pm 0.02$.

(c) $R \in [0.3, R_c \equiv 0.30710...]$ (8 *last points from the* $0H$ *interval*): $B(R) = b_1 (R_c - R)^{-b_2}$ where $b_1 = 2.26 \pm 0.08$ and $b_2 = 0.252 \pm 0.005$.

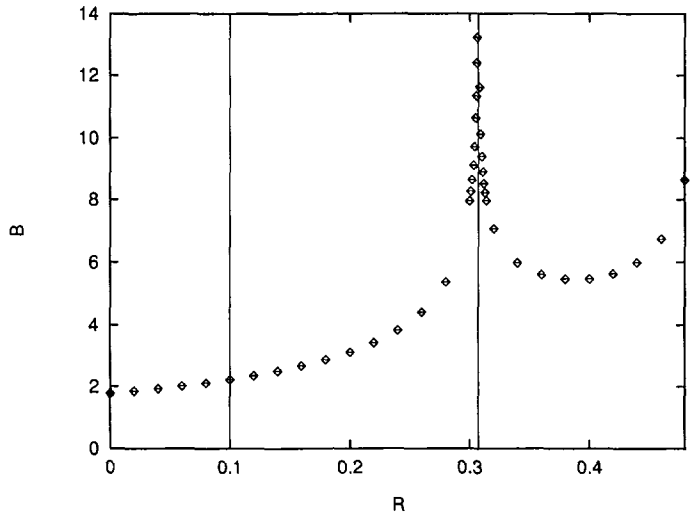

Fig. 4. Assymptotic values of $B(n)$ coming from the fit explained in Section 3I, as a function of the radius R.

(d) ∞H and $0H$ *intervals* (26 *points*): $B(R) = b_1 + b_2 R + b_3 (R_c - R)^{-b_4}$ where $b_1 = -3.5 \pm 0.7$, $b_2 = 1.3 \pm 0.7$, $b_3 = 4.1 \pm 0.6$ and $b_4 = 0.20 \pm 0.02$.

(e) D *interval* (18 *points*): $B(R) = (b_1 + b_2 R + b_3 R^2 + b_4 R^3)(R - R_c)^{-1/4}$ where $b_1 = -92.3 \pm 14.2$, $b_2 = 760.4 \pm 113.5$, $b_3 = -2036.0 \pm 298.2$ and $b_4 = 1825 \pm 258.1$.

(f) $R \in [R_c, 0.313]$ (*first* 8 *points from the D interval*): $B(R) = b_1 (R_c - R)^{-b_2}$ where $b_1 = 2.6 \pm 0.2$ and $b_2 = 0.22 \pm 0.01$.

From these fits we see that the B *critical* behavior near the radius $R \simeq R_c$ is given by a power law divergence with a critical exponent between 0.20 and 0.25.

II. The KS Entropy

Figure 5 shows similar plot as Fig. 3 for the Kolmogorov–Sinai entropy defined by Eq. (2.2). In this case it is more dramatic how after a few collisions the asymptotic value is reached. But, anyway, we have carried out a similar analysis as in the precedent case. The resulting asymptotic values are plotted in Fig. 6 and Fig. 7. We see that the KS entropy is not a monotonic function on R except in the $0H$ region in which it decreases with R. In the infinite horizon region, the inclusion of a sublattice of scatterers while keeping the infinite horizon topology, increases the entropy with respect the pure square lattice of scatterers i.e., $R = 0$. This

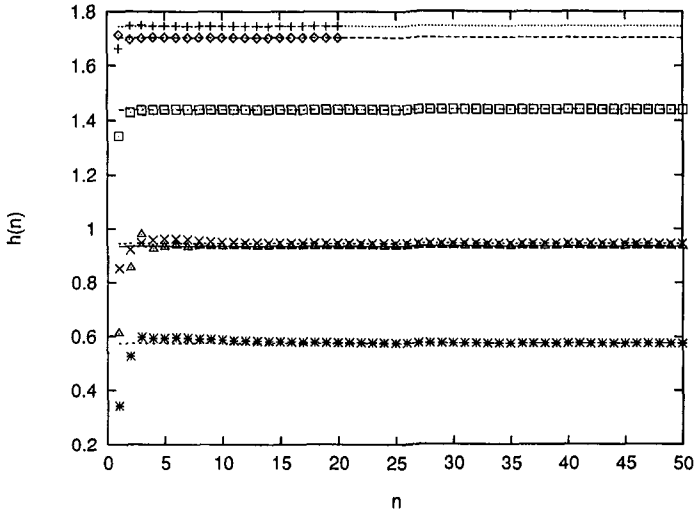

Fig. 5. $h(n)$ given by Eq. (2.2) as a function of n for different radius (from top to bottom): $R = 0.10, 0.0, 0.20, 0.30, 0.40$ and 0.48. The lines are the corresponding fits (see text).

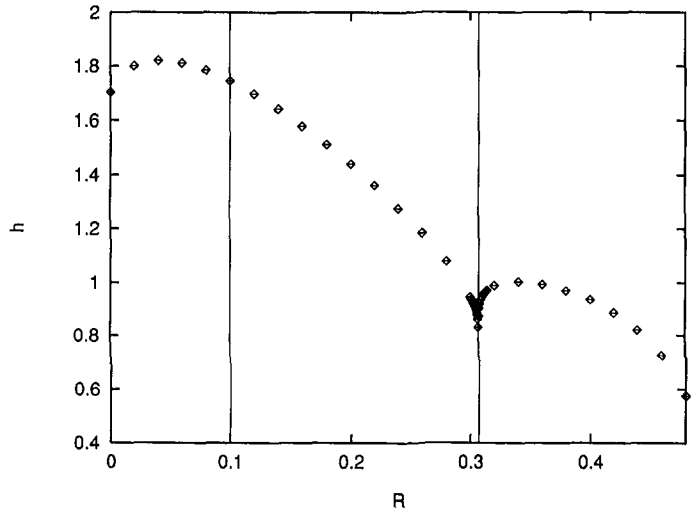

Fig. 6. The Kolmogorov–Sinai entropy computed from the assymptotic values of $h(n)$ coming from the fit explained in Section 3I, as a function of the radius R.

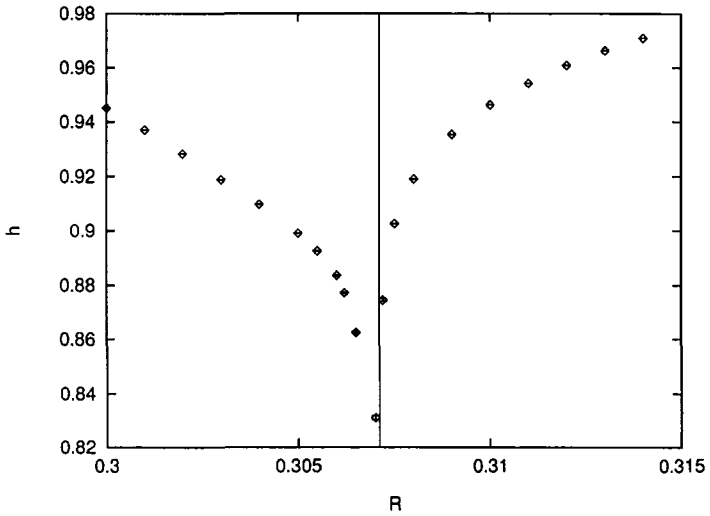

Fig. 7. Detailed behavior of the Kolmogorov–Sinai entropy around the critical radius $R_c = 0.3071...$ which separates the Diamond topology from the zero horizon one.

possibly means that the corresponding Marcov Partition will be more complicated with respect the $R = 0$ one. When the infinite horizon window is closed, the KS entropy becomes a, monotonic decreasing function on R in the $0H$ region. And therefore, by increasing R in this region, the Marcov Partition will be simpler. In the Diamond region the behavior is more involved. At the critical radius, R_c, the KS entropy reaches a. local minimum reflecting the fact that the trajectories spend most of the time at the Diamond vertex, i.e., they are localized at the phase space. By increasing R around R_c the KS entropy increases and reaches a maximum near $R = 0.34$. From there, the KS entropy decreases due to the smaller curvature of the scatterers. In Fig. 7 we see how the KS entropy behaves near the critical value R_c. It seems that is a continuous and no differentiable function in R_c.

III. The Mean Free Time

The computation of the mean free time give us the opportunity to check the goodness of our computer simulation. One may compute analytically its value and compare with the one obtained with the computer simulation. In fact, the analytical derivation is simple, the mean free time is given by

$$\tau = \int_M d\nu(x)\, \tau(x) \tag{3.2}$$

where M is the phase space defined by the coordinates $x=(r, \Phi)$ and $\tau(x)$ is the time that the particle takes to go from the initial position at x to the next collision point. Substituting $dv(x)=-(2P)^{-1}\cos(\Phi)\,dr\,d\Phi$ into Eq. (3.2) we get:

$$\tau=(2P)^{-1}\int_G dt\,dr\,d\Phi(-\cos\Phi)=(2P)^{-1}\int_G dx\,dy\,d\varphi=\pi A/P \tag{3.3}$$

where G is the phase space available by the flow (see ref. 9), x, y and φ are the spatial coordinates and the angle that the particle velocity forms with the x-axis respectively. Finally, A is the available area for the particle and P is the perimeter of the obstacles.

Equation (3.3) would lead to

$$\tau=\frac{1-\pi(R^2+R'^2)}{2(R+R')} \qquad R+R'\leqslant\frac{1}{\sqrt{2}} \tag{3.4}$$

and

$$\tau=\pi\frac{1/8-lR\sin(\pi/4-\beta)/2-\alpha R'^2/2-\beta R^2/2}{\alpha R'+\beta R} \qquad R+R'\geqslant\frac{1}{\sqrt{2}} \tag{3.5}$$

where

$$\alpha=\frac{\pi}{4}-\cos^{-1}\left(\frac{l^2+R'^2-R^2}{2lR'}\right) \tag{3.6}$$

$$\beta=\frac{\pi}{4}-\cos^{-1}\left(\frac{l^2+R^2-R'^2}{2lR}\right) \tag{3.6}$$

and $l=1/\sqrt{2}$ in our case.

Figures 8 and 9 represent the mean free time and its mean square displacement, σ_τ, for different R. In the ∞H region we see how the mean square displacement is finite which is against its expected infinite value. This is so because our algorithm discard the collisions which take more that 100 units of time. That is, in Eq. (2.4) all $\tau_i(n-1, n)$ are finite.

The dotted curve in Fig. 8 and Fig. 9 is the numerical solution of Eqs. (3.4) and (3.5). As we see, the formulas fits almost exactly the experimental data except in the neighborhood of the critical radius where the set of trajectories that spend many time *crossing* the vertex have a macroscopical influence on the value numerically obtained of the mean free time. One may think on doing larger computer simulations with more collisions but,

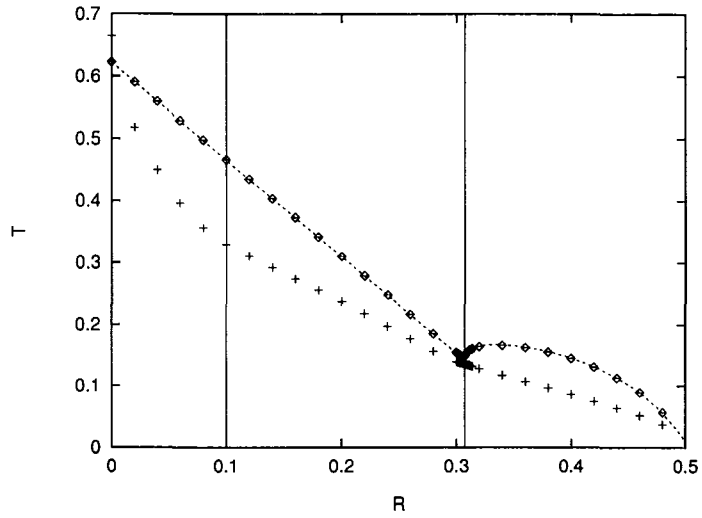

Fig. 8. Mean free time (diamond symbols) and its mean square displacement (plus symbols) as a function of R.

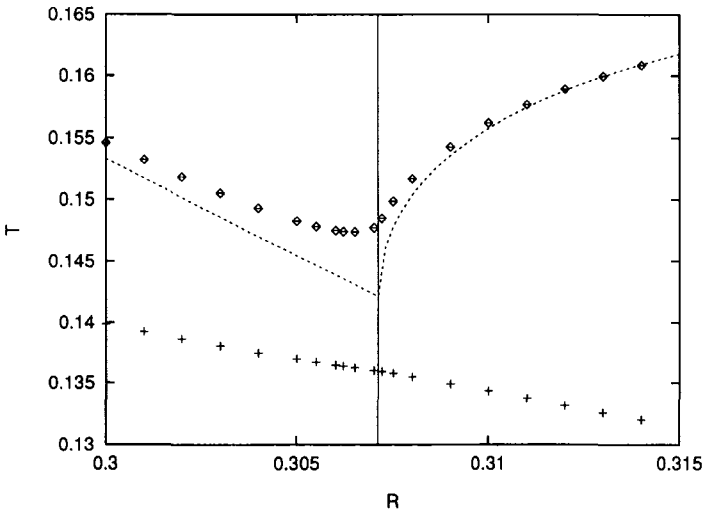

Fig. 9. Detailed behavior of the Mean free time (diamond symbols) and its mean square displacement (plus symbols) near the critical radius $R_c = 0.3071....$

as we discussed at the beginning of Section 3, there is an inherent limitation on this systems. The precision of the computer and the system chaoticity, limits to a maximum of about 50 collisions per evolution. It is clear that near R_c it is needed far more collisions in order to study the critical behavior cleanly. The present status of computer technology prevent us to study with confidence that region.

We have also carried out several linear fits to our data for the mean square displacement of τ:

(i) $0.1 \leqslant R \leqslant 0.3055$ (11 *points*): $\sigma_\tau(R) = d_1 + d_2 R$ where $d_1 = 0.426 \pm 0.001$ and $d_2 = -0.956 \pm 0.006$.

(ii) $R_c \leqslant R \leqslant 0.5$ (18 *points*): $\sigma_\tau(R) = d_1 + d_2 R$ where $d_1 = 0.306 \pm 0.001$ and $d_2 = -0.553 \pm 0.004$.

(iii) $0.3 \leqslant R \leqslant 0.315$ (20 *points*): $\sigma_\tau(R) = d_1 + d_2 R$ where $d_1 = 0.304 \pm 0.001$ and $d_2 = -0.549 \pm 0.005$.

Let us remark the linear behavior of the mean square displacement of τ. In particular, from the fits (ii) and (iii) we can conclude that the linear behavior of the D region *invades* the $0H$ region up to $R \simeq 0.3$. This behavior has a slope of about $-1/2$ while the corresponding to the $0H$ region (fit i)) has the slope of $\simeq -1$.

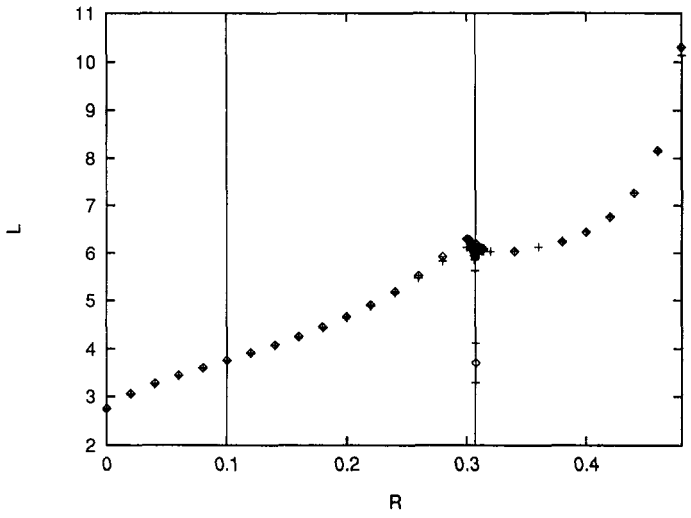

Fig. 10. Lyapunov exponent as a function of R computed by using Eq. (1.13) (diamond symbols) and the Abramov's formula (plus symbols).

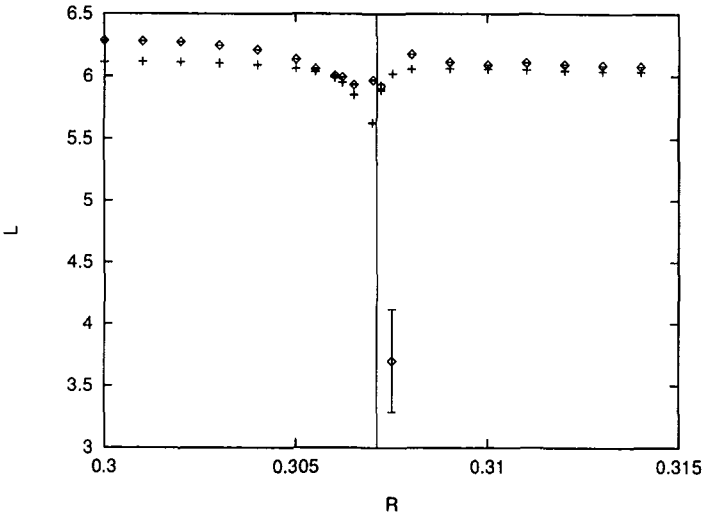

Fig. 11. Detailed behavior of the Lyapunov exponent near R_c computed by using Eq. (1.13) (diamond symbols) and the Abramov's formula (plus symbols).

IV. The Lyapunov Exponent

Figures 10 and 11 show the behavior of the Lyapunov exponent as computed by Eq. (1.13). In practice no difference has been found between both methods of computing L except near R_c where the convergence of Eq. (1.13) is much worse and leads to uncontrolled fluctuation of the nonlinear fits explained in Section 3I (see Fig. 11). The Lyapunov exponent increases with R from $R=0$ up to $R\simeq 0.3$. It reaches there a kind of plateau and decreases slightly near R_c. From R_c is increases a little bit and again it reaches a new tableau from which it increases with R. From the above analysis it seems that, again, the Lyapunov exponent is a continuous but not differentiable function around R_c.

4. CONCLUSIONS

The main goal of this paper was to make a generic numerical study of the influence of geometry in Billiards for some typical dynamic magnitudes as the mean curvature, the Kolmogorov–Sinai entropy, the mean free time and the Lyapunov exponent. In particular we have studied the effect in these magnitudes of the transitions between the Diamond, the zero horizon and the infinite horizon geometries. We have found that the transition

between OH and ∞H is smooth and no pathologies appear. In contrast, the transition between D and OH is much more interesting. First, the mean curvature seems to diverge around the critical radius which separate both geometries, R_c, with an exponent approximated equal to 1/4. Second, the latter divergence influences the KS entropy behavior but not the mean free time one whose analytical formula is well known. The KS entropy seems to be a continuous hut not differentiable function in R_c.

ACKNOWLEDGMENTS

I thank Prof. G. Gallavotti to introduce me in this class of very interesting problems. I thank to one of the referees for the explanation of how to derive the analytic formula for the mean free time (3.4), (3.5) and (3.6). This work was supported by the spanish agency DGICYT (PB91-0709), Junta de Andalucía (PAI) and the European Union under the Human Capital and Mobility program ERBCHRXCT940460. The author is indebted to Prof. J. L. Lebowitz for partial support through grants NFS-DMR92-18903 and AFOSR-F49620-92-J-0015.

REFERENCES

1. P. L. Garrido and G. Gallavotti, Billiards Correlation Functions, *J. Stat. Phys.* **76**:549–585 (1994).
2. G. Gallavotti, Lectures on the billiards, in "*Dynamical systems, theory and applications*," Lecture notes in Physics, Vol. 38, Springer-Verlag, Berlin, 1975, ed. J. Moser, p. 236–295; G. Gallavotti, *Problemes Ergodiques de la Mechanique Classique*, Enseignement du 3ème cycle de la Physique en Suisse Romande.
3. Ya. Sinai, Dynamical systems with elastic reflections, Ergodic properties of dispersing billiards, *Russ. Math. Surv.* **25**:137–189 (1970).
4. N. I. Chernov, New Proof of Sinai's formula for the entropy of hyperbolic billiard systems, application to Lorenz gases and Bunimovich stadiums, *Func. Anal. Appl.* **25**:204–219 (1991).
5. G. Benettin, Power-law behavior of Lyapunov exponents in some conservative dynamical systems, *Physica* **13B**:211–220 (1984).
6. G. Benettin and J. M. Strelcyn, Numerical experiments on the free motion of a point mass moving in a plane convex region: Stochastic transition and entropy, *Phys. Rev A* **17**:773–785 (1978).
7. B. Friedman, Y. Oono and I. Kubo, Universal Behavior of Sinai Billiard Systems in Small-Scatterer Limit, *Phys. Rev. Lett.* **52**:709–712 (1984).
8. J. P. Bouchaud and P. Le Doussal, Numerical Study of a D-Dimensional Periodic Lorentz Gas with Universal Properties, *J. Stat. Phys.* **41**:225–248 (1985).
9. P. R. Baldwin, The billiard algorithm and KS entropy, *J. Phys. A* **24**:L941-L947 (1991).
10. P. R. Baldwin, Soft billiard systems, *Physica D*, **29**:321–342 (1988).